European Journal of Orthodontics, 2016, 569–576
doi:10.1093/ejo/cjv096
Advance Access publication 5 January 2016

Original article

Connecting the new with the old: modifying the combined application of Procrustes superimposition and principal component analysis, to allow for comparison with traditional lateral cephalometric variables

Hans L. L. Wellens and Anne M. Kuijpers-Jagtman

Department of Orthodontics and Craniofacial Biology, Radboud University Nijmegen Medical Centre, The Netherlands

Correspondence to: Hans L. L. Wellens, Department of Orthodontics and Craniofacial Biology, Radboud University Nijmegen Medical Centre, 309 Tandheelkunde, PO Box 9101, 6500 HB Nijmegen, The Netherlands. E-mail: wellens.hans@telenet.be

Summary

Objective: The combination of generalized Procrustes superimposition (GPS) and principal component analysis (PCA) has been hypothesized to solve some of the problems plaguing traditional cephalometry. This study demonstrates how to establish the currently unclear relationship between the shape space defined by the first two principal components to the ANB angle, Wits appraisal, and GoGnSN angle, and to elucidate possible clinical applications thereof.
Methods: Digitized landmarks of 200 lateral cephalograms were subjected to GPS and PCA, after which the sample mean shape was deformed along/parallel to principal components (PC) 1 and 2, recording the ANB, Wits, and GoGnSN value at each location. Trajectories were then calculated through the PC1–PC2 space connecting locations with the same values. These were finally utilized to renormalize the PC1–PC2 space.
Results: The trajectories for the Wits appraisal were almost straight and parallel to PC1. Those for the ANB angle were angled approximately 20 degrees downward relative to PC1, with a more accentuated curvature. The GoGnSN curves were mildly angled relative to the PC2 axis, their curvature increasing slightly with increasing PC1 scores. By combining the aforementioned trajectories, it was possible to delineate the region of the PC1–PC2 shape space which would be regarded as normodivergent and skeletal Class I in traditional cephalometry. Geometric distortion could be avoided by assigning patients the ANB, Wits, or GoGnSN value of the sample mean shape, deformed to the patient's position within the PC1–PC2 plot.
Conclusion: The methodology successfully relates the shape space resulting from the GPS–PCA results with traditional cephalometric variables.

Introduction

Several recent studies have found the impact of cephalometrics on clinical practice to be rather limited (1–7). In fact, a 2013 meta-analysis by Rischen *et al.* (7) stated that 'cephalograms are not routinely needed for treatment planning in Class II malocclusions'; conclusions mirrored in a similar study by Durão *et al.* (6) who, in view of the very small number of high quality cephalometric studies meeting their (stringent) inclusions criteria, concluded that 'lateral cephalometric radiographs have been used without adequate scientific evidence', and that 'there is an urgent need to improve lateral cephalometry's diagnostic efficiency and therapeutic efficacy' (6). This might explain why, in order to allocate patients to study groups,

© The Author 2016. Published by Oxford University Press on behalf of the European Orthodontic Society. All rights reserved.
For permissions, please email: journals.permissions@oup.com

many researchers opt to combine several cephalometric variables (8–10), add dental and/or facial criteria (11–14), or even forego the former completely in favour of the latter (15–20). Intriguingly, several of the aforementioned studies are randomized controlled trials, which are considered to represent the highest standard among research designs (14–20).

Two-dimensional lateral cephalometry is indeed burdened with many technical problems (21, 22), such as image enlargement, blurring, and structural doubling or shrouding (22–24), while 'geometrical distortion' may play a role as well (22). The latter has frequently been associated with the ANB angle (25) and Wits appraisal (26–28), whereby the ANB angle has been reported susceptible to changes in the relative antero-posterior position of point N (29), relative bimaxillary protrusion or retrusion (30), and changes in midfacial height (31), allowing patients with the same mandibulomaxillary relationships to exhibit differing ANB values. The same holds true for rotations of the mandibulomaxillary complex relative to the skull base (27, 28) and vertical dento-alveolar dimensional changes (32). The Wits appraisal was found to be highly sensitive to changes in the cant of the occlusal plane (33). It therefore seems geometrical distortion is linked to the inter-individually highly variable nature of the reference landmarks and planes included in the aforementioned cephalometric analyses. This might be clarified further by considering the following analogy: when applying the ANB angle, orthodontists essentially attempt to triangulate intermaxillary relationships, much like land surveyors do. However, whereas the latter utilize external reference points of which the location (and elevation) is known exactly (e.g. 'benchmarks') (34), orthodontists implicitly assume that the patient's reference structures are 'located normally enough' to ensure the validity of the measurements performed. The aforementioned analogy would also suggest there is little merit in attempting to solve lateral cephalometry's problems by 'moving around the surveyor's tripod' to a different patient-specific reference point or plane.

In view of the aforementioned problems, some authors proposed applying Procrustes superimposition and principal component analysis (PCA) to lateral cephalometry (35, 36). Generalized Procrustes superimposition (GPS) (37–40) is an iterative mathematical algorithm involving the subsequent centring, scaling, and rotation of digitized landmark configurations, minimizing the distance between corresponding landmarks using the least squares criterion (Figure 1). As a result, GPS allows for the assessment of shape differences (40–42), whereas PCA uncovers the directions (in multidimensional space) in which the superimposed configurations vary most (39, 41, 42). When applying GPS and PCA to a set of commonly used lateral cephalometric landmarks, the resulting first and second principal components (PCs) were found to predominantly describe variation in the vertical (dolichofacial versus brachyfacial morphology) and antero-posterior dimensions (Class II versus Class III), respectively (36, 43) (Figure 2). When plotting PC1 versus PC2, the resulting graph might be construed as a map, of which each point characterizes a particular patient's vertical and horizontal skeletal makeup in terms of PC scores on the *x*- (PC 1) and *y*-axis (PC 2) (Figure 3). The higher/lower an individual's PC score, the more this patient differs morphologically from the sample mean configuration, which is located at the origin of the axis system (e.g. the more high angle, low angle, retrognathic, or prognathic this patient is). Because 'inter-patient distance' in the PC1–PC2 shape space may be utilized as a measure of morphological similarity (39, 41) (patients located closer together are more similar morphologically), the underlying distribution of the PC scores may be used to establish cut-off points for cephalometric analysis: a logical approach would be to designate those patients belonging to the central portion of the distribution of PC1 scores [e.g. PC1 mean ± 1 standard deviation (SD)] as being normodivergent, and of the PC2 scores as being skeletal Class I.

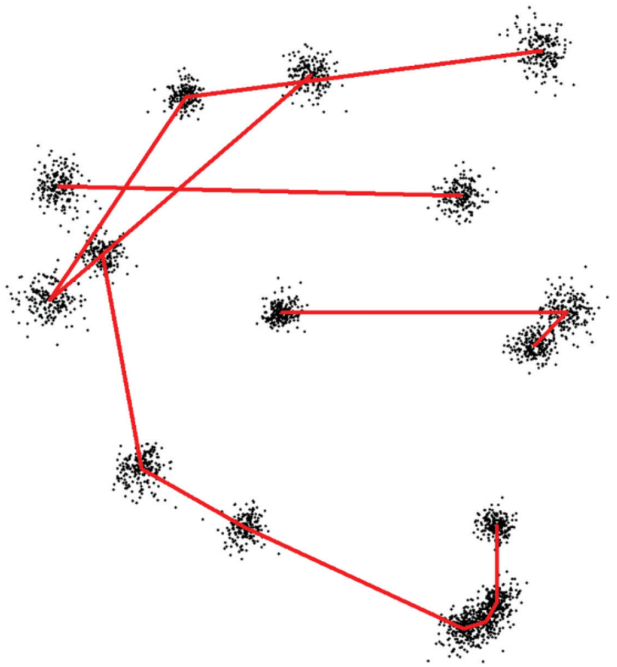

Figure 1. Generalized Procrustes superimposition of 16 skeletal landmarks (n = 200). GPS involves centring, scaling, and rotating the configurations in order to minimize the distance between the corresponding landmarks (using the least squares criterion), thus allowing for the assessment of shape. The sample mean shape is shown in red.

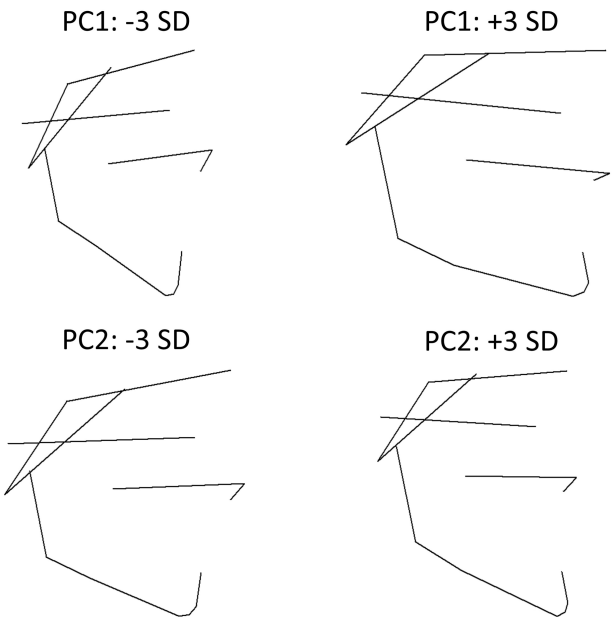

Figure 2. Deformation of the sample mean shape (depicted in red in Figure 1) of ±3 SD along the first (upper left and right panes) and second principal components (PCs) (lower left and right panes). These represent 'directions of greatest shape variation' (in decreasing order), along which the sample mean shape may be deformed for visualization purposes. The first PC represents dolichofacial versus brachyfacial morphology, whereas the second one characterizes retrognatism versus prognatism.

One of the main advantages of this population-driven approach is that the principal components it is based upon are derived from the co-ordinate data directly, irrespective of orthodontic preferences (or biases). This however implies that the first and second PCs might therefore include shape variance that is not related to the established (albeit ill-defined) orthodontic concepts to which they bear a striking resemblance: vertical growth pattern (PC1) and sagittal discrepancy (PC2) (Figure 2). Furthermore, the loss of a clear link between the GPS–PCA approach and the more familiar traditional cephalometric measures might be construed as a disadvantage: it is unclear how, if at all, both approaches might be related to one another. It might be beneficial if the advantages of the GPS–PCA approach could somehow be combined with the familiarity and utility of the traditional cephalometric measures, without reintroducing geometric distortion.

The aims of this proof-of-concept study therefore were to demonstrate a methodology for relating the shape space defined by the first two principal components to the 'traditional' cephalometric concepts of sagittal discrepancy (represented by the ANB angle and Wits appraisal) and vertical growth pattern (represented by the GoGnSN angle) while avoiding geometric distortion, and to illustrate how the currently proposed methodology might find clinical application.

Methodology

Because we aimed to allocate study participants to the experimental groups based upon the underlying distribution of the PC scores, the required sample size was based on an estimation of the number of subjects present in the tails of a normally distributed sample. Because about 16 per cent of this distribution is located in each tail (more than 1 SD away from the mean), a sample size of about 200 patients was estimated to be required in order to obtain about 30 subjects in each tail.

Two hundred consecutive lateral cephalometric radiographs (107 males, mean age: 12.8 years, SD: 2.2, range: 7.4–19.1; 93 females, mean age: 13.2 years, SD: 1.7, range 8.3–19.6) were therefore collected from the private practice of the first author (Table 1). The following inclusion criteria were applied: only pre-treatment radiographs, absence of craniofacial syndromes, only Caucasian patients, only radiographs taken in occlusion, and absence of gross movement artifacts. Patients had to be between 7 and 20 years old to be included in the sample.

All images were collected using a Planmeca Proline XC (Planmeca Oy, Helsinki, Finland) by the first author, using appropriate settings and a standardized technique. The radiographs were then loaded in Viewbox (dHal software version 4.0.1.7, Kifissia, Greece), in order to identify the position of 16 skeletal landmarks (Figure 4). Cephalometric enlargement was compensated for during the digitizing process. The obtained coordinates were then exported to R (http://www.r-project.org) for further processing.

The digitized skeletal coordinates of the pooled sample were superimposed using GPS (Figure 1) (39, 41, 44), and stereometrically projected onto tangent space (39, 45), after which the sample mean shape was calculated. The GPS superimposed and projected landmark coordinates were then subjected to PCA (42, 46), rendering the principal component scores and their standard deviations (Figure 3). In order to establish a relationship between the first two

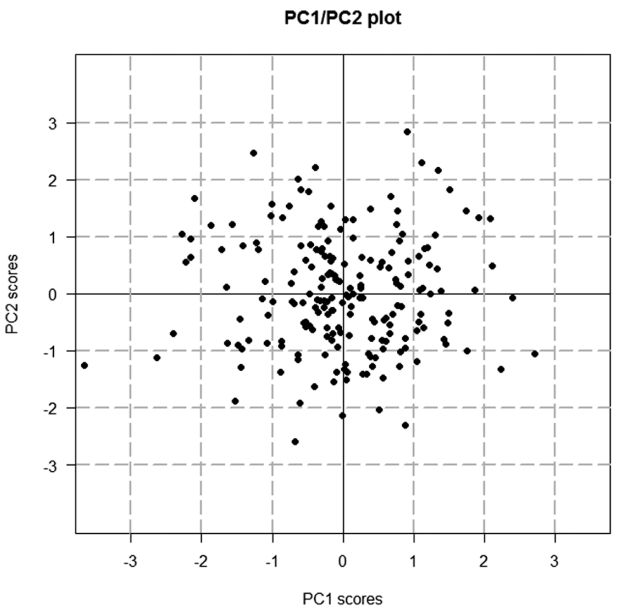

Figure 3. Plot of the first and second PCs (*x*-axis and *y*-axis, respectively), resulting from the PCA. The dots indicate where this sample's subjects are located within the PC1–PC2 space, whereby perpendicular projections onto the *x*- and *y*-axis represent the corresponding PC1 and PC2 scores, respectively. The sample mean shape is located at the origin of the axis system, while the dashed grey lines indicate the standard deviations. Referring to Figure 2, low PC1 scores (i.e. patients located more to the left in the plot) indicate a high angle growth pattern, whereas the reverse is true for high scores (i.e. brachyfacial morphology). Patients located higher in the PC1–PC2 plot (i.e. exhibiting higher PC2 scores) are more prognathic compared to patients with lower scores.

Table 1. Age distribution of the sample ($n = 200$).

	n	Mean	SD	Min	Max
Male	107	12.8	2.2	7.4	19.1
Female	93	13.2	1.7	8.3	19.6
Pooled	200	13.0	2.0	7.4	19.6

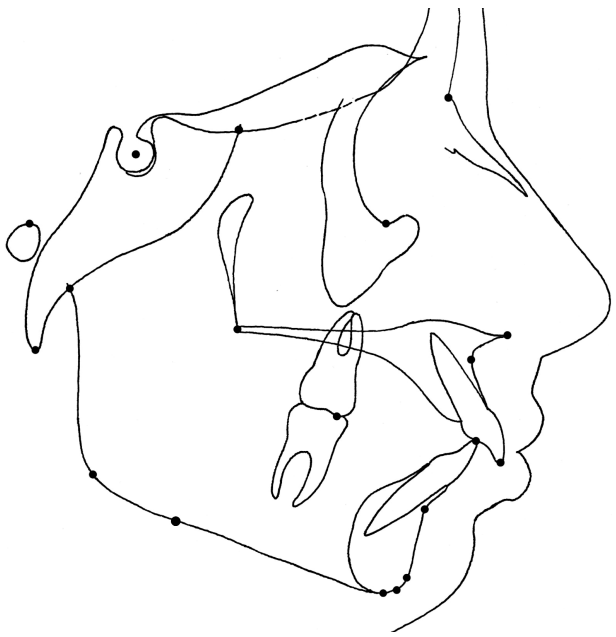

Figure 4. Digitized landmarks.

principal components on the one hand, and vertical growth pattern/sagittal discrepancy on the other hand, the sample mean shape was deformed from −3.5 to 3.5 SD, perpendicular or parallel to the *x*-(PC1) and *y*-axis (PC2) in 101 × 101 steps, recording the deformed sample mean shape's ANB angle, Wits appraisal (representing measures of sagittal discrepancy), and GoGnSN angle (as a proxy for sagittal discrepancy) in the process. The PC1–PC2 space (Figure 3) was thus sampled in terms of the three aforementioned traditional cephalometric measures at 10.201 discrete positions. Because the occlusal plane landmarks were excluded from the Procrustes analysis, their position in the deformed sample mean shape had to be extrapolated, by deforming the sample mean shape resulting from a GPS *with* occlusal plane landmarks to the same position in the PC1–PC2 space, and performing a thin plate spline (TPS) deformation (47) of the deformed configuration with occlusal plane landmarks on the one without them.

We then calculated trajectories through the PC1–PC2 space which would compensate for any observed changes in the Wits appraisal and ANB angle accompanying changing PC1 scores. These were determined by moving along the *y*-axis in 101 vertical steps between 3.5 and −3.5 SD PC2. At each vertical position, the space was sampled horizontally in 101 steps between −3.5 and 3.5 SD PC1. At each horizontal position, the corresponding deformed sample mean shape's ANB and Wits appraisal values were calculated. The latter two values were then compared to those exhibited by the deformed sample mean shape located at the same vertical level on the *y*-axis (e.g. same PC2 score). In case of differing values, we then calculated the vertical offset required to match the Wits appraisal or ANB angle of the deformed sample mean shape on the *y*-axis. The resulting trajectories therefore connected configurations exhibiting the same ANB or Wits values, but with varying GoGnSN angles. Using the same methodology, similar trajectories were calculated to compensate for any changes in GoGnSN values associated with changing PC2 scores.

Finally, we attempted to renormalize the PC1–PC2 space in order to obtain straight, orthogonal trajectories in the renormalized GoGnSN-ANB angle or GoGnSN-Wits appraisal space. In order to accomplish this, a 11 × 11 transformation matrix was defined, based upon the intersections of the compensation curves calculated earlier. Because the corresponding non-compensated coordinates were known as well, we were able to perform a TPS deformation (47), calculating the new patient coordinates based upon the matrices of compensated and non-compensated positions within the PC1–PC2 space.

Results

The sample's demographic data is presented in Tables 1 and 2. As evident from the heat map of the PC1–PC2 space in Figure 5, for the same value of PC2, low PC1 values (i.e. dolichofacial morphology) were associated with higher ANB values (yellow color), and higher PC1 values (i.e. brachyfacial morphology) with lower ANB values (in red). This can clearly be observed in Supplementary Animation 1. For the same PC2 value, high PC scores (prognathic morphology) were associated with smaller GoGnSN values, whereas lower scores (e.g. retrognathic shape) were linked to larger values (Supplementary Animation 2).

Table 2. Distribution of the pooled sample's ANB angle, Wits appraisal, and GoGnSN angle ($n = 200$).

	Mean	SD	Min	Max
ANB (°)	4	2.1	−2.8	8.6
Wits (mm)	3.0	3.3	−6.4	14.0
GoGnSN (°)	31.3	5.6	17.3	47.8

The diagonal curves in Figure 6A connect configurations exhibiting identical ANB values: when moving along them from left to right, the resulting deformed sample mean shape's GoGnSN angle changes from high to low, without concomitant change in the ANB value (Supplementary Animation 3). Contrary to the diagonal curves in Figure 6A, the corresponding trajectories for the Wits appraisal were found to be almost straight, and virtually parallel to the PC1 axis (Figure 6B, Supplementary Animation 4). The 'vertical' curves in Figure 6C connect configurations exhibiting identical GoGnSN values: moving along these from top to bottom, the resulting configurations morph from Class III to Class II, with no accompanying change in the GoGnSN angle (Supplementary Animation 5). The thicker black curves in the three aforementioned figures delineate the regions of the PC1–PC2 plot which would be regarded as skeletal Class I (Figure 6A and 6B) and mesofacial (Figure 6C), respectively based upon the distribution of the underlying PC scores (PC score mean ± 1 SD).

Figure 7A and 7B illustrate the TPS deformation grid (in red), constructed in order to renormalize the PC1–PC2 space. The corresponding original PC1–PC2 co-ordinate grid is depicted in grey. Supplementary Animation 6 provides a visual representation of the outer boundaries of the TPS deformation grid for the GoGnSN-Wits space. The aim of this renormalization was to obtain straight, orthogonal trajectories in the resulting, GoGnSN-Xdiff space. The recalculated, post-TPS patient scores are depicted in Figure 8. Please note that the renormalized axes are no longer expressed in PC scores, but in the corresponding GoGnSN and ANB or Wits standard deviation values. Patients located on the same horizontal level exhibit very similar (but not necessarily identical, see below) ANB or Wits values, whereas patients aligned vertically will have very similar GoGnSN

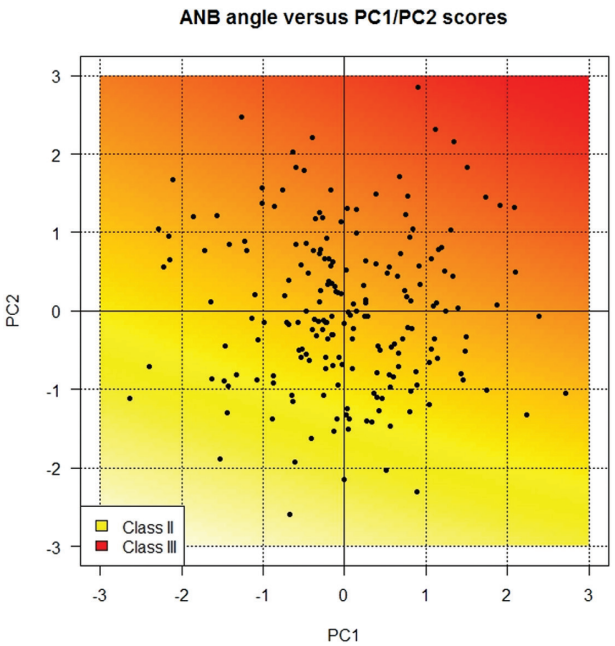

Figure 5. Heat map of the PC1–PC2 space. The colours represent the ANB values found at 10 201 discrete positions within this space. Yellow and red indicate higher and lower ANB values, respectively.

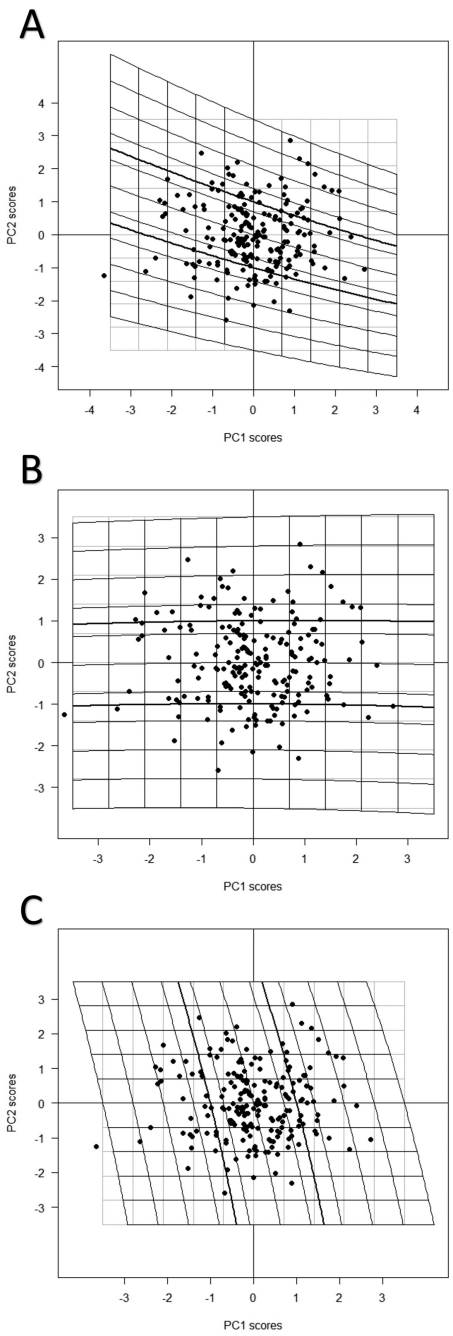

Figure 6. (A) PC1–PC2 plot, depicting the calculated trajectories within the PC1–PC2 space connecting locations with the same ANB measurements. Configurations located on the same trajectory therefore share the same ANB angle, albeit with differing degrees of facial divergence. The thick diagonals delineate the region of the PC1–PC2 plot which would be regarded as skeletal Class I (according to the ANB angle), based upon the distribution of the underlying PC scores (PC score mean ± 1 SD). All curves are angled downward approximately 20 degrees relative to the PC1 axis. (B) PC1–PC2 plot, depicting the calculated trajectories connecting locations with the same Wits appraisal values. The thick diagonals delineate the region of the PC1–PC2 plot which would be regarded as skeletal Class I according to the Wits appraisal, based upon the distribution of the underlying PC scores (PC score mean ± 1 SD). All curves are parallel to the PC1 axis and only very slightly curved. (C) PC1–PC2 plot, depicting the calculated trajectories connecting locations with the same GoGnSN measurements. The thick diagonals delineate the region of the PC1–PC2 plot which would be regarded as normodivergent, based upon the distribution of the underlying PC scores (PC score mean ± 1 SD). The calculated trajectories are mildly angled relative to the PC2 axis, their curvature increasing slightly with increasing PC1 scores.

values. As was to be expected, the renormalized co-ordinate system is no longer oriented along the direction of maximum variation.

Discussion

Contemporary cephalometric variables describe separate, discontinuous aspects of craniofacial morphology and typically do not lend themselves to straightforward graphical representation (21). This leaves the orthodontist with the intellectually challenging task of re-integrating the different variables into a cohesive mental picture, subsequent diagnosis and final treatment plan; a task which may be compounded further by diagnostic confusion, if the application of different cephalometric variables to the same morphological trait leads to differing or even contradictory diagnoses (8, 22, 48). This can clearly be observed in Figure 9, where the blue dots represent the present sample's patients for whom the diagnoses according to the ANB angle and Wits appraisal disagree (i.e. Class I/II or I/III, 47 patients), whereas the red dots represent patients with contradictory diagnostic outcomes (i.e. Class II/III, one patient). The combination of GPS and PCA offers a potential solution to this predicament, because the underlying distribution of the resulting PC2 scores allows for objective patient classification based upon their mandibulomaxillary relationships (Figures 2 and 3 and Supplementary Animation 2). The same holds true for the PC1 scores and vertical growth pattern (Figures 2 and 3 and Supplementary Animation 3), although some reservations apply (discussed further in the text). Our aim was to assess what might be learned, both clinically and theoretically, from establishing a relationship between the 'new' GPS/PCA approach and 'traditional' cephalometric variables, preferably without reintroducing geometric distortion in the process.

This was accomplished by deforming the sample mean shape to a large number of pre-determined positions within the PC1–PC2 space, and measuring the deformed sample mean shape's ANB angle, Wits appraisal, and GoGnSN angle in the process. The resulting PC1–PC2 plot may be used as an objective tool for comparing the performance of the latter: Figure 9 depicts those regions of the PC1–PC2 plot which would be regarded as Class I according to the ANB angle and the Wits appraisal (determined by calculating trajectories within the PC1–PC2 plot connecting configurations with the same ANB angle and Wits appraisal and GoGnSN angle; Figure 6A–6C). Intriguingly, the 'Class I band' for the ANB angle (mean ± 1 SD, in between the blue curves in Figure 9) was found to be rotated clockwise relative to that for the Wits appraisal (shaded in green, Figure 9), resulting in areas within the PC1–PC2 plot where patients should ideally be diagnosed differently without exception (e.g. Class I/II or Class I/III, areas shaded in grey in Figure 9). In other words, Figure 9 suggests that diagnostic confusion is unavoidable if both ANB and Wits are used for assessing mandibulomaxillary relationships (irrespective of which cut-off points are used), because they measure different morphological traits.

The fairly uniform distribution with which instances of diagnostic confusion seems to occur over the PC1–PC2 plot (Figure 9) might be explained by geometric distortion: individual variations in the location of the measurement's reference landmarks and planes tend to distort the corresponding cephalometric value (29–33). A potential approach to preventing geometric distortion might therefore be to not measure these variables directly, but instead assign patients the corresponding value of the sample mean shape, deformed to the patient's position within the PC1–PC2 plot (measurement 'by proxy'), thus applying the same 'ruler' to all patients. As such, it represents a generalization of the approach proposed earlier by Wellens (22). If this measurement methodology is adopted, Figure 6A and 6B suggest

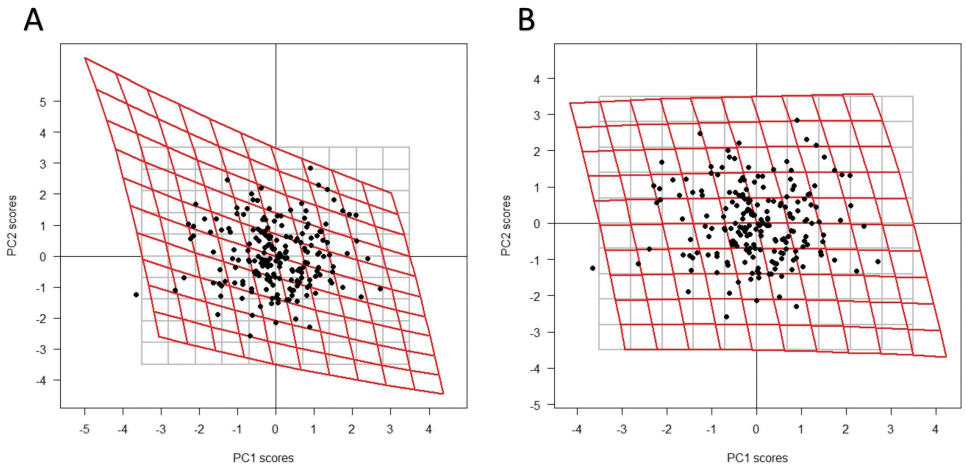

Figure 7. (A) Thin plate spline deformation grid (in red), constructed in order to renormalize the PC1–PC2 space in terms of the GoGnSN and ANB angle. The corresponding original PC1–PC2 coordinates are depicted in grey. TPS calculates a smooth deformation from the red towards the grey grid, and interpolates the resulting patient positions in the process. (B) Thin plate spline deformation grid (in red), constructed in order to renormalize the PC1–PC2 space in terms of the GoGnSN angle and Wits appraisal. The corresponding original PC1–PC2 coordinates are depicted in grey.

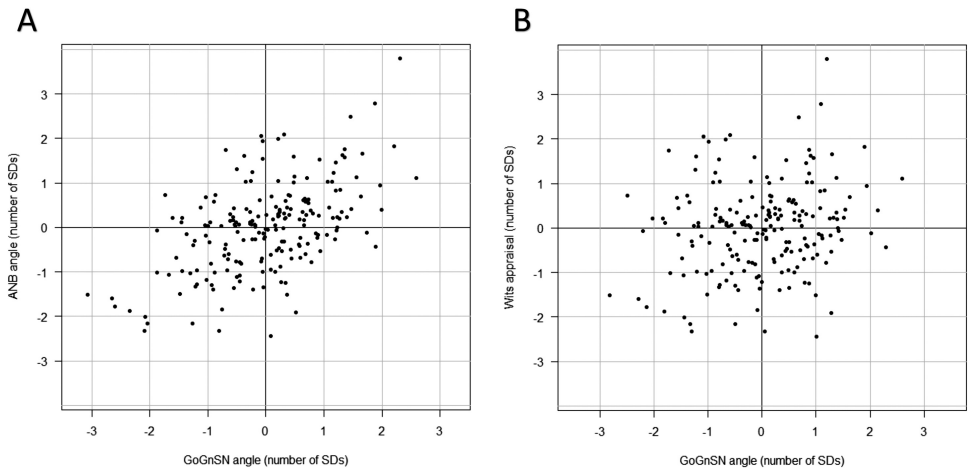

Figure 8. (A) Post-TPS patient coordinates. The new *x* and *y*-axes represents the GoGnSN and ANB angle values, respectively (in SD). (B) Post-TPS patient coordinates. The new *x* and *y*-axes represent the GoGnSN angle and Wits appraisal values, respectively (in SD).

that the 'Wits analysis by proxy' might be a more useful measure than the corresponding ANB angle: Because the trajectories connecting configurations with the same Wits appraisal are almost straight, and virtually parallel to the PC1 axis (Figure 6B), it would seem the 'Wits analysis by proxy' is better aligned with the directions of greatest variation, compared to the corresponding ANB measurement.

As evident from Figure 7A and 7B, it is possible to renormalize the PC1–PC2 plot using a TPS deformation, such that the compensation lines and curves from Figure 5A and 5B straighten out within the newly defined co-ordinate system. The latter is of course a largely cosmetic operation, although it may facilitate the visual appraisal of the inter-patient relationships in terms of the traditional cephalometric values.

To insure the PCA only reflected skeletal variational patterns, we opted not to include the highly variable occlusal plane landmarks in the GPS. The position of these landmarks in the deformed sample mean shape therefore had to be interpolated using TPS deformation. Because pilot studies confirmed the reliability of this procedure, we felt it could be safely adopted. Furthermore, it is always possible to apply the calculated transformations to the complete configurations (including dental landmarks), in order to visualize the occlusal plane/incisors in the resulting (skeletal) Procrustes superimposition. Another possible criticism is that (currently) the methodology only takes into account the first two principal components. Although the remaining PCs indeed have an increasingly smaller influence on the patient's craniofacial shape (41), it may not necessarily be totally negligible. This would appear to pertain mostly to the GoGnSN angle, because the third and fourth PC seem to influence mainly the gonial angle, and will be investigated further in a follow-up investigation. Another possible critique pertains to the apparent complexity of the methodology, which should nevertheless be relatively straightforward to implement in clinical practice: upon digitizing the lateral cephalogram in a predetermined order, a computer program would use pre-supplied data (the reference sample's post-GPS coordinates, matrix of principal components, and the 'by proxy' ANB, Wits, and GoGnSN 'normal zones') to calculate the patient's principal component scores, visualize his/her position in the PC1–PC2 plot, and calculate the accompanying vertical and sagittal 'by proxy' measurements directly, without having to repeat all calculations mentioned in the methodology. Apart from supplying 'distortion free' cephalometric

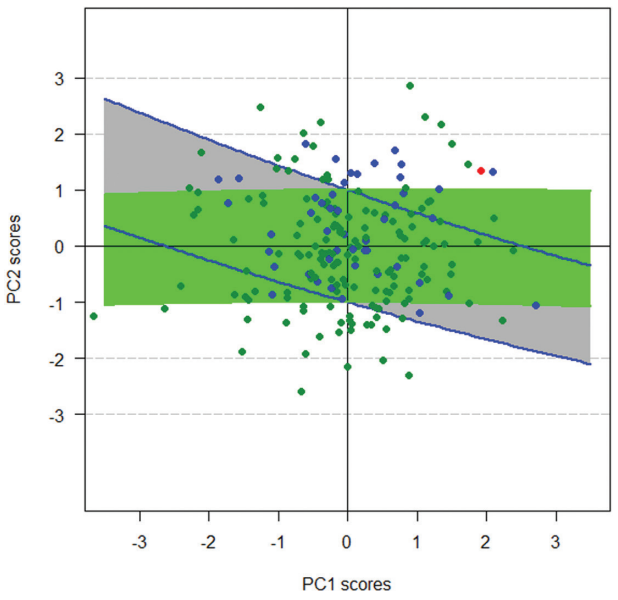

Figure 9. PC1–PC2 plot, depicting the concordance between the diagnoses according to the (traditional) ANB angle and Wits appraisal. Diagnostic agreement is indicated by a green dot (Class I/Class I), disagreement in blue (Class I/II, Class I/III), and contradiction in red (Class II/III). The green area represents the region of the PC1–PC2 plot which would be regarded as Class I according to the Wits appraisal. The corresponding region for the ANB angle is located in between the two blue curves. The grey areas depict the regions of the PC1–PC2 plot where patients should ideally be diagnosed differently without exception (Class I/II or Class I/III).

values, the software might also provide surgical visual treatment objectives: by perpendicularly projecting a patient's position in the PC1–PC2 plot upon the *x*-axis in Figure 3, the corresponding configuration at that location may be calculated. This corresponds to the craniofacial a shape the corresponding patient would exhibit if his/her first PC score were average (e.g. mesofacial). A similar approach may be used for projections on the *y*-axis.

Conclusion

The proposed methodology demonstrates how to establish the relationship between the first two principal components resulting from GPS/PCA, and conventional cephalometric variables such as the ANB angle, Wits appraisal, and GoGnSN angle. It also suggests how the latter measurements may be performed within this space without re-introducing geometric distortion, by assigning patients the corresponding value exhibited by the sample mean shape deformed to the patients position within the PC1–PC2 plot (measurement 'by proxy'). The Wits 'by proxy' measurements were found to be better aligned with the directions of maximum variation, compared to the corresponding ones for ANB angle.

Supplementary material

Supplementary material is available at *European Journal of Orthodontics* online.

Acknowledgements

We would like to sincerely thank Professors Demetrios Halazonetis and Ellen A. BeGole for their extremely valuable advice, Professor Fred Bookstein for proofreading the manuscript, and the reviewers for their helpful comments.

References

1. Atchison, K.A., Luke, L.S. and White, S.C. (1991) Contribution of pretreatment radiographs to orthodontists' decision making. *Oral Surgery, Oral Medicine, and Oral Pathology*, 71, 238–245.
2. Han, U.K., Vig, K.W.L., Weintraub, J.A., Vig, P.S. and Kowalski, C.J. (1991) Consistency of orthodontic treatment decisions relative to diagnostic records. *American Journal of Orthodontics and Dentofacial Orthopedics*, 100, 212–219.
3. Hansen, K. and Bondemark, L. (2001) The influence of lateral head radiographs in orthodontic diagnosis and treatment planning. *European Journal of Orthodontics*, 23, 452–453.
4. Nijkamp, P.G., Habets, L.L., Aartman, I.H. and Zentner A. (2008) The influence of cephalometrics on orthodontic treatment planning. *European Journal of Orthodontics*, 30, 630–635.
5. Devereux, L., Moles, D., Cunningham, S.J. and McKnight, M. (2011) How important are lateral cephalometric radiographs in orthodontic treatment planning? *American Journal of Orthodontics and Dentofacial Orthopedics*, 139, e175–e181.
6. Durão, A.R., Alqerban, A., Ferreira, A.P. and Jacobs, R. (2015) Influence of lateral cephalometric radiography in orthodontic diagnosis and treatment planning. *The Angle Orthodontist*, 85, 206–210.
7. Rischen, R.J., Breuning, K.H., Bronkhorst, E.M. and Kuijpers-Jagtman, A.M (2013) Records needed for orthodontic diagnosis and treatment planning: a systematic review. *PLoS ONE*, 8, e74186.
8. Kim, Y. (1978) Anteroposterior dysplasia indicator—adjunct to cephalometric differential-diagnosis. *American Journal of Orthodontics and Dentofacial Orthopedics*, 73, 619–633.
9. Ishikawa, H., Nakamura, S., Iwasaki, H. and Kitazawa, S. (2000) Seven parameters describing anteroposterior jaw relationships: postpubertal prediction accuracy and interchangeability. *American Journal of Orthodontics and Dentofacial Orthopedics*, 117, 714–720.
10. Bingmer, M., Özkan, V., Jo, J.M., Lee, K.J., Baik, H.S. and Schneider, G. (2010) A new concept for the cephalometric evaluation of craniofacial patterns (multiharmony). *European Journal of Orthodontics*, 32, 645–654.
11. Ge, Y.S., Liu, J., Chen, L., Han, J.L. and Guo, X. (2012) Dentofacial effects of two facemask therapies for maxillary protraction. *The Angle Orthodontist*, 82, 1083–1091.
12. Moreno Uribe, L.M., Vela, K.C., Kummet, C., Dawson, D.V. and Southard, T.E. (2013) Phenotypic diversity in white adults with moderate to severe Class III malocclusion. *American Journal of Orthodontics and Dentofacial Orthopedics*, 144, 32–42.
13. Moreno Uribe, L.M., Howe, S.C., Kummet, C., Vela, K.C., Dawson, D.V. and Southard, T.E. (2014) Phenotypic diversity in white adults with moderate to severe Class II malocclusion. *American Journal of Orthodontics and Dentofacial Orthopedics*, 145, 305–316.
14. Baysal, A. and Uysal, T. (2014) Dentoskeletal effects of Twin Block and Herbst appliances in patients with Class II division 1 mandibular retrognathy. *European Journal of Orthodontics*, 36, 164–172.
15. Tulloch, J.F., Phillips, C., Koch, G. and Proffit, W.R. (1997) The effect of early intervention on skeletal pattern in Class II malocclusion: a randomized clinical trial. *American Journal of Orthodontics and Dentofacial Orthopedics*, 111, 391–400.
16. Keeling, S.D., Wheeler, T.T., King, G.J., Garvan, C.W., Cohen, D.A., Cabassa, S., McGorray, S.P. and Taylor, M.G. (1998) Anteroposterior skeletal and dental changes after early Class II treatment with bionators and headgear. *American Journal of Orthodontics and Dentofacial Orthopedics*, 113, 40–50.
17. Wheeler, T.T., McGorray, S.P., Dolce, C., Taylor, M.G. and King, G.J. (2002) Effectiveness of early treatment of Class II malocclusion. *American Journal of Orthodontics and Dentofacial Orthopedics*, 121, 9–17.
18. Tulloch, J.F.C., Proffit, W.R. and Phillips, C. (2004) Outcomes in a 2-phase randomized clinical trial of early Class II treatment. *American Journal of Orthodontics and Dentofacial Orthopedics*, 125, 657–667.
19. O'Brien, K. *et al.* (2009) Early treatment for Class II Division 1 malocclusion with the Twin-block appliance: a multi-center, randomized, controlled

trial. *American Journal of Orthodontics and Dentofacial Orthopedics*, 135, 573–579.
20. Dolce, C., McGorray, S.P., Brazeau, L., King, G.J. and Wheeler, T.T. (2007) Timing of Class II treatment: skeletal changes comparing 1-phase and 2-phase treatment. *American Journal of Orthodontics and Dentofacial Orthopedics*, 132, 481–489.
21. Moyers, R.E. and Bookstein, F.L. (1979) The inappropriateness of conventional cephalometrics. *American Journal of Orthodontics*, 75, 599–617.
22. Wellens, H. (2009) Improving the concordance between various anteroposterior cephalometric measurements using Procrustes analysis. *European Journal of Orthodontics*, 31, 503–515.
23. Baumrind, S. and Frantz, R.C. (1971) The reliability of head film measurements. *American Journal of Orthodontics*, 60, 111–127.
24. Baumrind, S. and Frantz, R.C. (1971) The reliability of head film measurements. *American Journal of Orthodontics*, 60, 505–517.
25. Steiner, C.C. (1953) Cephalometrics for you and me. *American Journal of Orthodontics*, 39, 729–755.
26. Jacobson, A. (1975) The "Wits" appraisal of jaw disharmony. *American Journal of Orthodontics*, 67, 125–138.
27. Jacobson, A. (1976) Application of Wits appraisal. *American Journal of Orthodontics and Dentofacial Orthopedics*, 70, 179–189.
28. Jacobson, A. (1988) Update on the Wits appraisal. *The Angle Orthodontist*, 58, 205–219.
29. Taylor, C.M. (1969) Changes in the relationship of nasion, point A, and point B and the effect upon ANB. *American Journal of Orthodontics*, 56, 143–163.
30. Freeman, R.S. (1981) Adjusting A-N-B angles to reflect the effect of maxillary position. *The Angle Orthodontist*, 51, 162–171.
31. Binder, R.E. (1979) The geometry of cephalometrics. *Journal of Clinical Orthodontics*, 13, 258–263.
32. Hussels, W. and Nanda, R.S. (1984) Analysis of factors affecting angle ANB. *American Journal of Orthodontics*, 85, 411–423.
33. Roth, R. (1982) The 'Wits' appraisal—its skeletal and dento-alveolar background. *European Journal of Orthodontics*, 4, 21–28.
34. *Benchmark (surveying)* (2015). Wikipedia, the Free Encyclopedia, February 19, 2015. http://en.wikipedia.org/w/index.php?title=Benchmark_(surveying)&oldid=647927071 (15 March 2015, date last accessed).
35. McIntyre, G.T. and Mossey, P.A. (2003) Size and shape measurement in contemporary cephalometrics. *European Journal of Orthodontics*, 25, 231–242.
36. Halazonetis, D.J. (2004) Morphometrics for cephalometric diagnosis. *American Journal of Orthodontics and Dentofacial Orthopedics*, 125, 571–581.
37. Goodall, C. (1991) Procrustes methods in the statistical analysis of shape. *Journal of the Royal Statistical Society. Series B (Methodological)*, 53, 285–339.
38. Bookstein, F.L. (1997) Landmark methods for forms without landmarks: morphometrics of group differences in outline shape. *Medical Image Analysis*, 1, 225–243.
39. Dryden, I.L. and Mardia, K.V. (1998) *Statistical Shape Analysis*. Wiley, Chichester, New York.
40. Kendall, D.G. (1977) The diffusion of shape. *Advances in Applied Probability*, 9, 428.
41. Zelditch, M.L., Swiderski, D.L. and Sheets, H.D. (2012) *Geometric Morphometrics for Biologists: A Primer*. 2nd edn. Academic Press, Amsterdam, the Netherlands.
42. Hotelling, H. (1933) Analysis of a complex of statistical variables into principal components. *Journal of Educational Psychology*, 24, 417–441.
43. Wellens, H.L., Kuijpers-Jagtman, A.M. and Halazonetis, D.J. (2013) Geometric morphometric analysis of craniofacial variation, ontogeny and modularity in a cross-sectional sample of modern humans. *Journal of Anatomy*, 222, 397–409.
44. Gower, J.C. and Dijksterhuis, G.B. (2004) *Procrustes Problems*. Oxford University Press, Oxford, New York.
45. Claude, J. (2008) *Morphometrics with R*. 1st edn. Springer, New York.
46. Pearson, K. (1901) LIII. On lines and planes of closest fit to systems of points in space. *Philosophical Magazine Series 6*, 2, 559–572.
47. Bookstein, F.L. (1989) Principal warps: thin-plate splines and the decomposition of deformations. *IEEE Transactions on Pattern Analysis and Machine Intelligence*, 11, 567–585.
48. Demisch, A., Gebauer, U. and Zila, W. (1977) Comparison of three cephalometric measurements of sagittal jaw relationship: angle ANB, Wits appraisal and AB-occlusal angle. *Transactions of the European Orthodontic Society*, 2, 269–281.